lubricants

MDPI

Article

Comparison of Friction Properties of GI Steel Plates with Various Surface Treatments

Miroslav Tomáš [1,*], Stanislav Németh [2], Emil Evin [1], František Hollý [2], Vladimír Kundracik [2], Juliy Martyn Kulya [1] and Marek Buber [1]

[1] Department of Automotive Production, Faculty of Mechanical Engineering, Technical University of Košice, Mäsiarska 74, 040 01 Košice, Slovakia; emil.evin@tuke.sk (E.E.)
[2] USSE Research and Development, U.S. Steel Košice s.r.o., Vstupný Areál U.S. Steel, 044 54 Košice, Slovakia; snemeth@sk.uss.com (S.N.); fholly@sk.uss.com (F.H.); vkundracik@sk.uss.com (V.K.)
* Correspondence: miroslav.tomas@tuke.sk; Tel.: +421-55-602-3524

Abstract: This article presents the improved properties of GI (hot-dip galvanized) steel plates in combination with a special permanent surface treatment. The substrate used was hot-dip galvanized deep-drawn steel sheets of grade DX56D + Z. Subsequently, various surface treatments were applied to their surface. The coefficient of friction of the metal sheets without surface treatment, with a temporary surface treatment called passivation, and a thin organic coating (TOC) based on hydroxyl resins dissolved in water, Ti and Cr^{3+} were determined by a cup test. The surface quality and corrosion resistance of all tested samples were also determined by exposing them for up to 288 h in an atmosphere of neutral salt spray. The surface microgeometry parameters Ra, RPc and Rz(I), which have a significant influence on the pressing process itself, were also determined. The TOC deposited on the Zn substrate was the only one to exhibit excellent lubrication and anticorrosion properties, resulting in the lowest surface microgeometry values owing to the uniform and continuous layer of the thin organic coating compared to the GI substrate and passivation surface treatment, respectively.

Keywords: thin organic coating; galvanized steel; cup test; friction coefficient; corrosion resistance

check for updates

Citation: Tomáš, M.; Németh, S.; Evin, E.; Hollý, F.; Kundracik, V.; Kulya, J.M.; Buber, M. Comparison of Friction Properties of GI Steel Plates with Various Surface Treatments. *Lubricants* **2024**, *12*, 198. https://doi.org/10.3390/lubricants12060198

Received: 26 April 2024
Revised: 24 May 2024
Accepted: 28 May 2024
Published: 31 May 2024

Copyright: © 2024 by the authors. Licensee MDPI, Basel, Switzerland. This article is an open access article distributed under the terms and conditions of the Creative Commons Attribution (CC BY) license (https://creativecommons.org/licenses/by/4.0/).

1. Introduction

The formability of steel plates and the shape of the final parts made from them depend on factors such as the material (its mechanical properties and surface microgeometry) [1,2]; the forming die geometry (die clearance, radii of the punch and die) and microgeometry (roughness of contact surfaces) [3–5]; the technological parameters (temperature, strain rate, blank holding forces, contact pressure, etc.) [6–8]; the properties of the tool's material (hardness, chemical composition, structure) [9]; and the type and amount of lubricant used [10]. During the deep drawing process, the individual parameters change and their mutual interaction has an influence on the formability, which is largely influenced by the lubricant or lubrication strategy. Correct selection of the lubricant is therefore one of the fundamental factors that ensures either the quality of the deep drawing process or its result in the form of the stamped part itself [11,12].

The functions of the lubricant in the deep drawing process are usually of a different nature. In general, however, the role of the lubricant is to minimize the friction acting on the contact surfaces of the tool in order to achieve the greatest possible ductility and to take maximum advantage of all of the plastic properties of the material [13]. Lubricants must perform other functions, such as the protection of metal sheets against corrosion, easy application and the removal of surfaces when necessary [14]. Nowadays, novel tribological systems are being studied, such as using volatile medium-like liquid carbon dioxide (CO_2) and gaseous nitrogen, directly introduced into the friction zones during deep drawing. These alternatives aim to reduce environmental impacts and eliminate the need for post-forming cleaning processes [15]. Good adhesion and homogeneity of the lubricant on the

surface of the sheet must also be ensured from application through to transport, storage and processing. Lubricants must be stable in the pressing process as well as non-hazardous and their application should be cost-effective [16].

One possible way to obtain these properties for a specific area of the stampings produced is the development of coatings based on a combination of a zinc coating with an applied permanent thin organic coating. Such a coating should be compatible with all Zn coatings and remain on the metal sheets during pressing [17,18]. The low coefficient of friction obtained should allow for more uniform reshaping in tooling and for maximum use of the mechanical properties for sharper lines of the stampings [19,20]. The dry lubricant on the steel plates should meet the requirement of eliminating coating flaking and the need for additional oil, thus keeping the forming presses (the contact surfaces of the blank holder, punch and die) clean and ready for the next step of production [21]. A typical permanent coating consists of a coating–forming material (resin) and different types of additives (forming additives and corrosion inhibitors) [22–24] enhancing conductivity and/or corrosion protection [25].

An example of such surface treatment on Zn, Al-Zn, Al-Zn-Si, Mg-Al-Zn and other substrates is a thin organic coating (TOC). The coating contains a limited amount of inorganic Cr^{3+} and Ti components [26]. After drying, they form a thin dry film with a thickness from 0.8 to 1.7 µm (i.e., 1.0 to 2.0 g/m^2). The coating serves as a permanent protection for galvanized sheet metal in transparent and colored versions [26–29]. Steel sheets with a thin organic coating currently provide an effective solution for applications where traditional passivated or oiled galvanized material is used, particularly in corrosion-sensitive conditions. The advantages and functional properties of the coating are excellent corrosion resistance and the absence of hexavalent chromium, which is RoHS-compliant based on Directive 2011/65/EU of the European Parliament and the Council [30]. The coating improves the formability due to the lower coefficient of friction "f", whose value of less than 0.15 is strictly required by sheet metal fabricators, especially in the white goods sector. When forming sheet metal with such surface protection, there is no need to add any pressing oils as it is also compatible with subsequent joining processes (gluing, welding…). A thin organic coating is also characterized by AFP—anti finger print, i.e., fingerprint resistance. In addition, these coated steel sheets are suitable for painting without any pre-treatment, for interior and exterior use, as well as for exposed and unexposed parts of products. This coating has a wide range of applications: construction—profiles, electronics—TV panels and Hi-Fi systems, and others—furniture, air conditioning, appliances, etc. [25–29].

The tribological behavior of TOCs is being tested by different methods to evaluate the friction coefficient in dry/wet contact conditions. The modified scratch test is well suited to serve as a first screening method to compare the tribological performance of different types of thin organic permanent coatings for forming applications [31,32]. Pin-on-disc/ball-on-disc tests are useful when determining the friction coefficient of organic/inorganic coatings [33,34]. While the mentioned tests belong to the basic testing methods performed in laboratory conditions, the bending under tension test allows for the modeling of the friction conditions on the edge of the die [31,35,36]. More complex tests, involving real conditions in deep drawing/stretching processes, are the cup test and biaxial stretching test. In [37], the authors tested the formability of organic coated steel sheet metal by using the cup test and biaxial stretching, focusing on the fracture behavior of the coating during forming operations. A biaxial tension state showed a greater effect on the coating compared to a mixed compression–tension state, even if the crack development was demonstrated to be similar. By using the cup test, it is possible to model the stress of the contact surfaces during sheet metal forming [38]. The cup test offers a more CF-process-relevant determination approach for the prediction of the technological characteristics of the deep drawing process [39,40].

The aim of this paper is to study the tribological and corrosion properties of a thin organic coating (TOC) based on hydroxyl resins dissolved in water and compare them

with a standard Zn coating and a passivated one. All of these coatings were created on a standard drawing quality steel substrate.

2. Materials and Methods

2.1. Experimental Materials—Substrate and Coatings

This experimental study was carried out on 1.0 mm thick steel sheet specimens of deep-drawn grade DX56D + Z. Tested samples of hot-dip galvanized steel sheet (GI substrate) were used as the reference material with a Zn layer thickness of 80 g/m^2 (40/40 g/m^2). Further, for comparison, the same quality hot-dip Zn coating with an applied surface treatment called passivation (based on inorganic substances) and also the same Zn coating with the TOC in a white shade were used. It is a single-component product based on Ti and Cr^{3+}. All of these coatings were in the same condition "as delivered" [27].

Figure 1 depicts a selected region of the metallographic section of the sample with the TOC analyzed under an Olympus GX 71 light microscope (Olympus, Tokyo, Japan). The Zn layer thickness was from 5 to 7 µm on both the top and bottom of the steel substrate. The thickness of the organic coating was controlled during its application to the Zn substrate according to the titanium content of the coating and the thickness of the dry film on the surface of the Zn substrate.

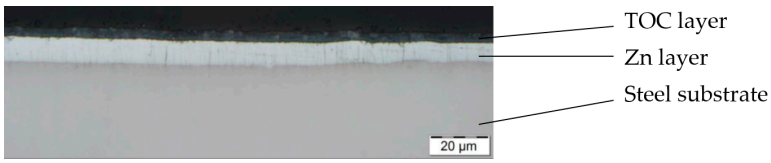
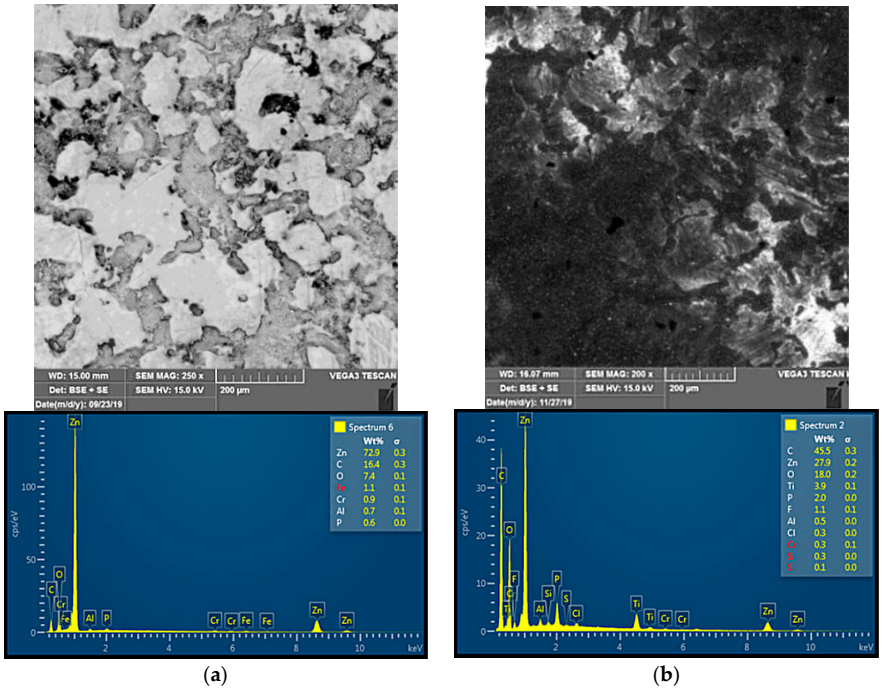


Figure 1. Cross-section of galvanized steel substrate with TOC layer.

The EDX/SEM analysis of the surface treatment (Figure 2b) confirmed a relatively stable chromium content in the range of 0.3 ± 0.1 wt%, which also corresponded with the required thickness of the coating applied. The uniform distribution of the pigment particles in the TOC after application to the steel sheet was also observed. The analysis was performed using a TESCAN VEGA 3 scanning electron microscope (TESCAN GROUP, a.s., Brno, Czech Republic) coupled with an OXFORD Instruments EDS analyzer.



(**a**) (**b**)

Figure 2. EDX analysis: (**a**) passivated GI coating; (**b**) GI coating with TOC.

The chemical composition of the substrate, which meets the prescribed limits of EN 10346 [41] (Table 1), was determined with an OBLF QSG 750 Analyzer (OBLF, Witten, DE, Germany) by using optical emission spectral analysis.

Table 1. Chemical composition of 1.0 mm thick substrate DX56D + Z (max. values) [wt%].

C	Mn	Si	P	S	Ti
0.12	0.6	0.5	0.1	0.045	0.3

2.2. Mechanical Properties of Substrate

The mechanical properties were determined by using a Zwick/Roell Z050 machine (Ulm, Germany) in the transversal direction (90°) to the rolling direction and meet the limits shown in Table 2. These properties were determined according to EN ISO 6892-1 [42], the normal anisotropy "r" was determined according to EN ISO 10113 [43] and the strain hardening exponent "n" was determined according to EN ISO 10275 [44] on standardized specimens (20 mm in width and 80 mm of original gauge length). The plastic strain ratio was determined at 20% of the engineering strain level and the strain hardening exponent was determined within the strain interval of 5% to uniform elongation A_g [42–44].

Table 2. Mechanical properties of 1.0 mm thick substrate DX56D + Z in transversal direction (90°).

	$R_{p0.2}$ (YS) [MPa]	R_m (UTS) [MPa]	A_{80} [%]	r [−]	n [−]
Measured	175 ± 1.3	301 ± 1.1	43.5 ± 0.9	2.30 ± 0.03	0.23 ± 0.005
Required	120–180	260–350	39% min.	1.9 min.	0.21 min.

$R_{p0.2}$ (YS) is proof strength; R_m (UTS) is ultimate tensile strength; A_{80} is percentage elongation after fracture; r is plastic strain ratio; n is strain hardening exponent.

2.3. Cup Test

To determine the lubrication properties (the value of the friction coefficient on the contact surfaces of the die and the blank holder), the well-known formability test—the cup test—was used, which simulates the stresses on the material in a real deep drawing process [38–40]. This test can be used to describe the most frequent contacts in the tribological system between the tool (punch, blank holder, die), friction material (sheet metal specimen/product) and intermediate material (lubricant, oil, foil or permanent special coating on sheet metal)—Figure 3 [12,38].

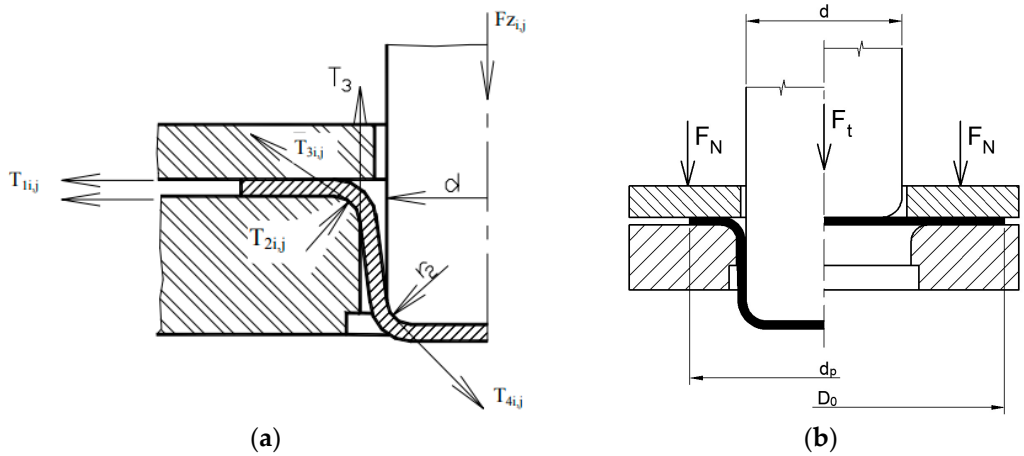


Figure 3. The principle of the cup test to determine the friction coefficient: (**a**) the friction forces during the cup test: $T_{1i,j}$ is the friction force under the blank holder, $T_{2i,j}$ is the normal force at the die radius, $T_{3i,j}$ is the friction force at the die radius and $T_{4i,j}$ is the friction force at the punch radius; (**b**) a schematic illustration of the cup test: F_N is the blank holder force and F_t is the drawing force [12,38].

The friction coefficient "f" of the tested specimens with different surface treatments was determined on the basis of the increase in the contact force and the subsequent results of the tensile forces. The coefficient of friction generally represents the ratio of the frictional force between two surfaces (press tool–sheet metal) and the load applied perpendicular to these surfaces. It should not be overlooked that the coefficient of friction depends not only on the condition of the surface (surface roughness, surface with or without lubricant) but also on other boundary conditions such as contact force, drawing speed, etc.

The cup test allows for the modeling of the tribological conditions at the contact surfaces of the tribo-system tool–lubricant–material, as they are carried out under semi-operational deep drawing conditions. Thus, this test is closer to the real deep drawing process and allows us to determine the friction coefficient under the blank holder. The friction coefficient "f" was determined for each type of surface (GI coating) specified as follows:

A—Reference GI coating (as supplied);

B—Passivated GI coating;

C—GI coating with the thin organic coating.

To determine the friction coefficient, a flat-bottomed punch with a diameter of ø 50 mm was used. Circular blanks with a constant diameter of 90 mm were cut out and subsequently subjected to plastic deformation on an Erichsen 145/60 hydraulic testing machine (Erichsen GmbH & Co. KG, Hemer, Germany). The blank holder force F_N represented loads of 10, 20, 30, 40 and 50 kN and the punch speed was kept constant (60 mm·min^{-1}) during the test. Ten cups were drawn for each level of the blank holder force. At these holding forces, the maximum drawing force F_t required to reshape the blank was recorded from the entire force course. Then, an average value of the drawing force and its standard deviation were calculated. After plotting F_t-F_N on a graph and interpolating the trend equation over these values, a linear relationship was obtained, where the angle under the curve represents the friction in the contact surfaces between the press tool and the sheet metal specimen. Thus, the evaluation method used a regression analysis where the slope of this linear trend line represents the value of the friction coefficient 'f' [12,40].

During the cup test (Figure 3), each blank holding force F_N corresponded to the maximum tensile force F_t—Figure 4a. A change in the blank holding force caused the maximum drawing force F_t to change. The graph shows that the relationship F_t—F_N is linearly dependent (curve 1, Figure 4b) and it can be approximated as follows [12,40]:

$$F_t = \text{Intercept} + \text{Slope} \cdot F_N, \quad (1)$$

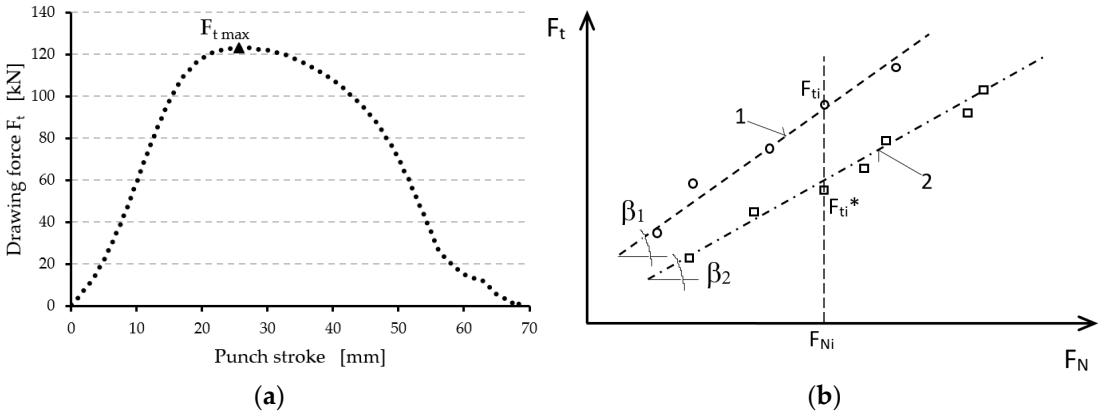


Figure 4. Evaluation of the cup test: (**a**) determination of the maximum drawing force F_t from the record of the force course; (**b**) determination of the friction coefficient for different lubricants [12,38,40].

The slope of the curve, given by the angle β_1, characterizes the friction conditions between the tool and the blank. Then, the friction coefficient is determined as follows:

$$f = \frac{\text{Slope}}{2} = \frac{\beta_i}{2} \quad (2)$$

In the case of a lubricant with improved frictional properties (lower coefficient of friction), we obtain lower drawing forces F_{Ti}* for the same blank holding force F_{Ni} and thus a new relationship F_{Ti}*—F_{Ni} (curve 2, Figure 4b). The slope of curve 2 (β_2) is less than the slope of curve 1 (β_1) and is proportional to the coefficient of friction between the tool and the blank.

2.4. Surface Microgeometry

Measuring the roughness parameters was carried out on a roughness measuring device, Hommel Tester T2000 (Hommelwerke, Schwenningen, Germany). Measurements of the roughness parameters Ra (arithmetic mean deviation of profile), RPc (peak count number) and Rz (maximum height of profile) were carried out on all sheet metal specimens from both sides of the blank (A side, B side) at five different points uniformly distributed on each specimen. Then, the average value of each evaluated parameter was calculated.

2.5. Corrosion Resistance according to ISO 9227

All tested specimens were placed in the SKBW 400 A-TR corrosion chamber (Liebisch GmbH & Co. KG, Bielefeld, Germany) and tested in an atmosphere of neutral salt spray (NSS) according to ISO 9227 [45]. A 5% sodium chloride solution (50 g/L ± 5 g/L of NaCl) was continuously sprayed onto the samples placed in the rack at an angle of 20° ± 5° to the vertical direction using an air nozzle at an ambient temperature T = 35 ± 2 °C. The accelerated corrosion test was carried out to detect discontinuous layers, such as pores and other defects, in certain metallic, organic, anodic oxide and conversion specialty coatings. The size of all tested specimens was 210 × 290 mm and the corrosion resistance of the coatings was evaluated based on the time until the appearance of white corrosion, evaluated after 5, 24, 48, 72, 96, 120, 144, 216 and 288 h spent in the corrosion chamber.

3. Results

The average values of the surface microgeometry parameters calculated from the five measured values on each side of the specimens are presented in Table 3 for each coating used in the experiment. As it is shown in the table, the reference "as supplied" GI coating showed an Ra value of 1.153 ± 0.170 µm, an Rz value of 7.028 ± 0.878 µm and an RPc value of 50.7 ± 10.0 cm^{-1} with a low difference when measured on each side of the steel sheet. The same tendency was noted for the GI passivated surface, with average values of Ra = 1.050 ± 0.132 µm, Rz = 6.754 ± 0.453 µm and RPc = 49.2 ± 5.6 cm^{-1}, and for the GI coating with the TOC, with average values of Ra = 0.934 ± 0.101 µm, Rz = 5.957 ± 0.505 µm and RPc = 48.5 ± 5.681 cm^{-1}. It can be concluded that the applied organic coating follows the morphology of the substrate surface, and the applied dry film microlayer influences the microgeometry of the coating by decreasing the coating roughness parameters Ra and Rz, while maintaining RPc at almost the same value.

The results of the drawing force measurement in the cup test for each coating are shown in Table 4. When the GI coating was lubricated by the oil during the cup test, the drawing forces ranged from 60.3 to 69.8 kN (Figure 5), with an increasing blank holder force, while the standard deviation was from 0.9 to 1.3 kN. Thus, a linear trend line that approximates the average values of the drawing forces predicts a friction coefficient f_{GI} = 0.119 with a Pearson correlation coefficient R = 0.999. The same tendency but a lower friction coefficient was found when the GI coating after passivation was used (dry friction): the drawing forces increased from 52.1 to 59.2 kN, with a standard deviation from 0.7 to 1.0 kN. The friction coefficient was f_{GIpass} = 0.091, with a Pearson correlation coefficient

R = 0.999. The lowest drawing forces were measured when the GI coating with the TOC was tested: the drawing forces increased from 41.7 to 46.1 kN, with a standard deviation from 2.0 to 2.3 kN. Thus, the lowest friction coefficient was determined as $f_{GI + TOC}$ = 0.053 with a Pearson correlation coefficient R = 0.995. For each coating tested, a very good correlation between drawing force and blank holder force was determined.

Table 3. The average values of the surface microgeometry parameters measured at 90° to the rolling direction.

Title 1	Title 2	Ra [µm]		Rz [µm]		RPc [cm^{-1}]	
		A Side	B Side	A Side	B Side	A Side	B Side
GI coating	Average	1.286	1.020	7.646	6.410	54.6	46.8
	St.dev	0.111	0.091	0.610	0.640	13.0	4.3
		1.153 ± 0.170		7.028 ± 0.878		50.7 ± 10.0	
Passivated GI coating	Average	1.162	0.938	7.132	6.376	53.0	45.4
	St.dev	0.058	0.066	0.141	0.290	3.9	4.3
		1.050 ± 0.132		6.754 ± 0.453		49.2 ± 5.6	
GI coating with TOC	Average	1.022	0.846	6.332	5.582	49.6	47.4
	St.dev	0.038	0.045	0.179	0.436	4.3	4.1
		0.934 ± 0.101		5.957 ± 0.505		48.5 ± 5.681	

Table 4. The deep drawing forces measured in the cup test for each blank holder force.

Blank Folder Force F_N [kN]	Deep Drawing Force Ft [kN]		
	GI	GI Passivated	GI + TOC
10	60.3 ± 0.9	52.1 ± 0.9	41.7 ± 2.0
20	62.7 ± 1.1	53.8 ± 0.7	43.1 ± 2.0
30	65.4 ± 1.3	55.6 ± 1.0	44.1 ± 2.3
40	67.5 ± 1.1	57.7 ± 0.8	44.9 ± 2.1
50	69.8 ± 0.9	59.2 ± 0.9	46.1 ± 2.0
Slope	0.238	0.182	0.105
Friction coefficient	0.119	0.091	0.053
R^2	0.9989	0.9985	0.9893

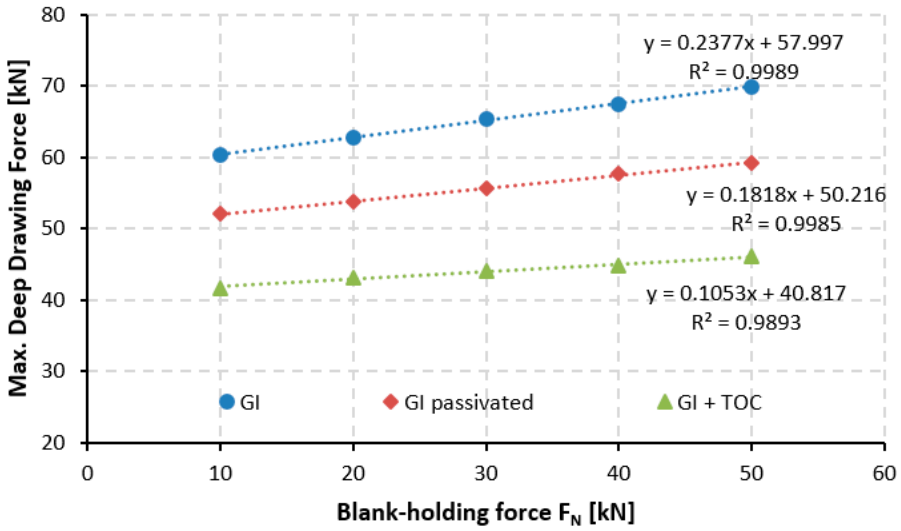


Figure 5. Regression analysis of measured drawing forces.

The adhesion of the coating to the substrate was evaluated after the cup test through visual inspection and microscopic analysis. No flaking or separation of the organic TOC from the substrate was observed on the surface of the cups (Figure 6; Canon EOS 100D 18 MPx with EFS 18–55 mm; Canon, Tokyo, Japan) at different F_N blank holding force loads. Even at the maximum loading force F_N = 50 kN, there was no adhesion of the coating or its elements to the drawing tool's contact surfaces (drawing die radius or blank holder area). Thus, good adhesion of the TOC was observed.

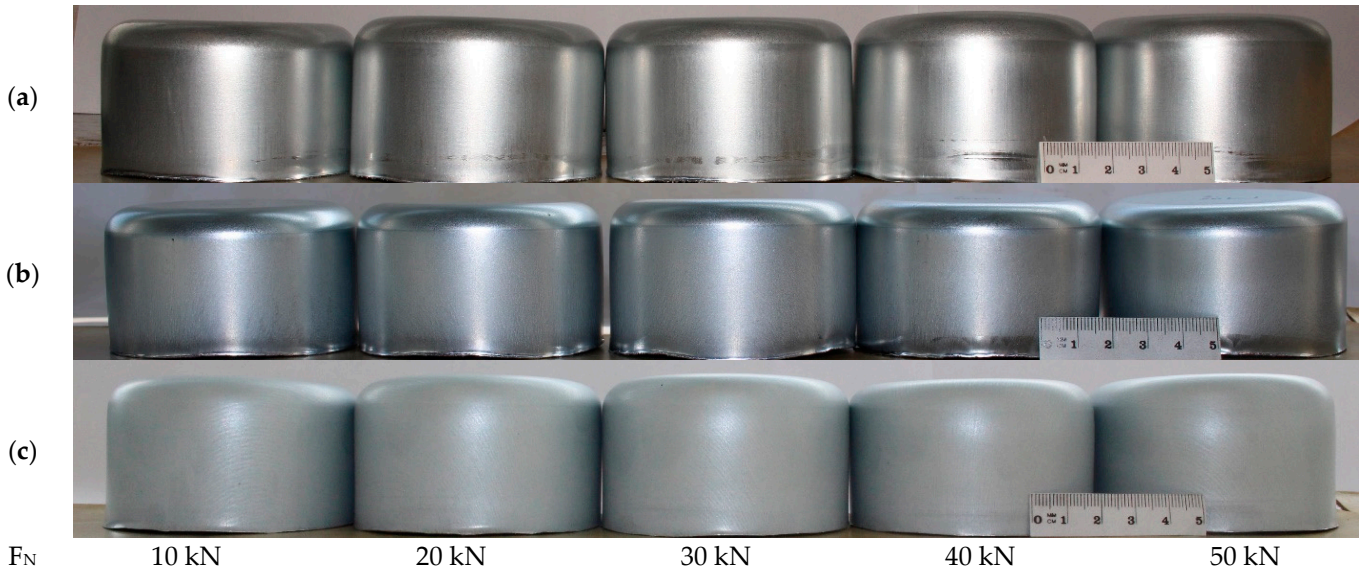


Figure 6. Adhesion of coating to GI substrate after cup test: (**a**) GI oiled; (**b**) GI passivated; (**c**) GI−TOC.

The results of the corrosion test after a selected number of hours in the corrosion chamber are shown in Figure 7. Based on the test results, it can be concluded that white corrosion appeared on the surface of the samples with the conventional GI coating without surface treatment during the first hours of exposure to a neutral atmosphere of salt solution. Surface treatment of the GI coating by means of standard passivation showed better corrosion resistance, i.e., the observation of white corrosion started after more than 24 h. The GI coating with the TOC showed the best corrosion resistance in relation to the compared coatings, with no observation of white corrosion for up to 144 h. Since the corrosion resistance limit for the TOC is set at 72 h (customer quality standard), the coated specimens still have a sufficient margin.

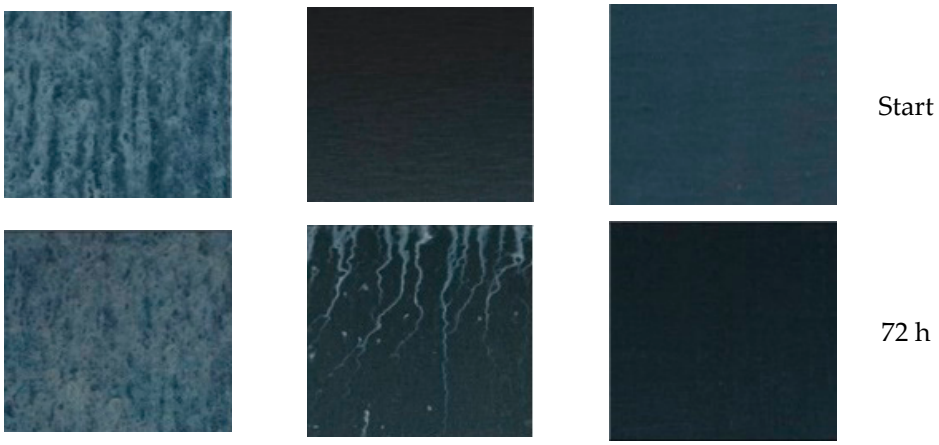


Figure 7. *Cont.*

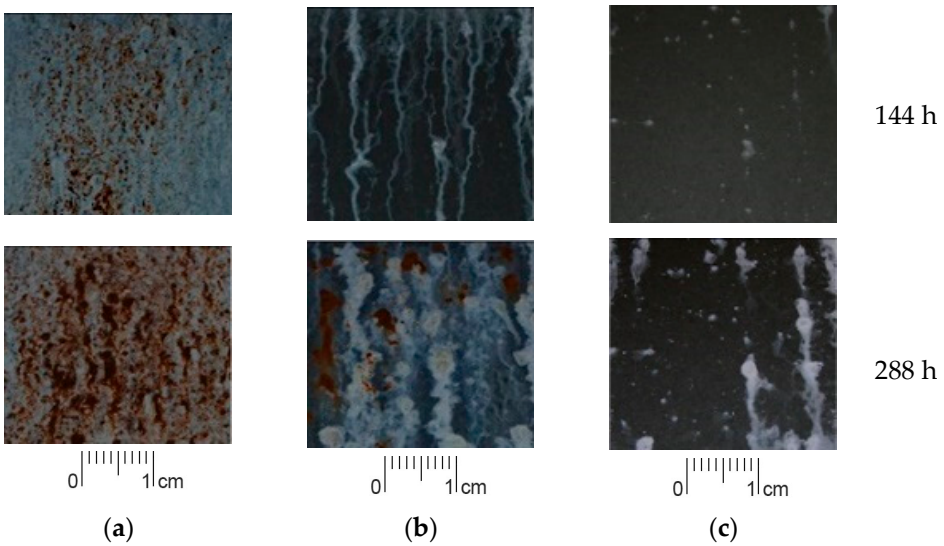


Figure 7. Kinetics of corrosion resistance of different coatings: (**a**) GI coating as reference one (as supplied); (**b**) passivated GI coating; (**c**) GI coating with TOC.

Figure 8 illustrates the comparison of time to white corrosion appearance between examined coatings.

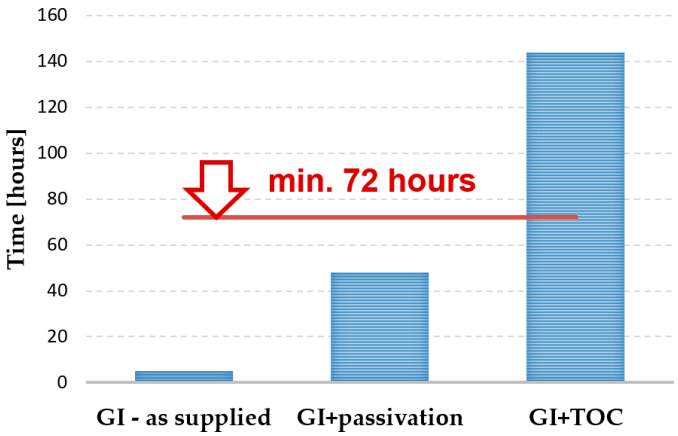


Figure 8. Comparison of time to white corrosion for examined coatings.

4. Discussion

From the perspective of steel sheet surface morphology, it can be concluded that the applied passivation and organic coating follow the morphology of the substrate surface, and the applied dry organic microlayer influences the microgeometry of the coating by decreasing the coating roughness parameters Ra and Rz. After passivation, the roughness of the passivated GI surface was Ra = 1.050 ± 0.132 µm and Rz = 6.754 ± 0.453 µm, while applying the organic coating decreased the roughness to Ra = 0.934 ± 0.101 µm and Rz = 5.957 ± 0.505. The surface morphology after phosphating depends on the deposition temperature and the concentration of the additives [46,47]; the self-lubricating coating can smooth the surface of the galvanized steel sheet and decrease the surface roughness of the galvanized steel sheet [48].

For all tested samples, GI as supplied, passivated GI and GI + TOC, the value of the friction coefficient determined by the cup test was f < 0.15 (the required parameter f_{max} for final sheet metal processors is 0.15). Thus, for samples without surface treatment (GI), the value 0.119 was reached when oil was used as a lubricant, while for dry friction (no oil used) samples with passivation (GI + passivation), it was 0.091, and for samples with the thin organic coating (GI + TOC), the value was 0.053.

The effect of phosphating on lowering the friction coefficient was proven by Narayanan [49]. Shih tested pre-phosphated DDQ and AHSS steels by using the bending under tension test and the results showed much a lower friction coefficient compared to without the pre-phosphated coating [50]. But, in a dry condition, phosphate coatings usually do not have inherent low-friction properties and they have no practical effect on the friction coefficient [21,51]. Carlsson [31,52] evaluated the friction coefficient of organic permanent coatings by using different basic tests. They achieved the lowest friction coefficient for a pure organic coating in the modified scratch test and pin-on-disc test within the range from 0.06 to 0.11, while in the bending under tension test, the friction coefficient varied from 0.16 to 0.17. Liu et al. [48] also studied self-lubricating coatings from the view of the influence of surface roughness on the friction coefficient and wear. Their results showed that within the range from 0.857 to 1.629 µm of the Ra value, the friction coefficient varied from 0.073 to 0.108 when measured by the reciprocating friction and wear tester. It may be concluded that when comparing the friction coefficient of 0.053 measured by the authors for the TOC (based on hydroxyl resins dissolved in water) by using the cup test, this value is comparable to the results mentioned. Thus, the positive effect of the TOC on lowering the friction coefficient in the deep drawing process can be elucidated.

The corrosion test showed the enhanced properties of the TOC applied on the GI steel compared to the passivated surface. The results are supported by other authors. Podjuklova et al. [53] proved the enhanced short-term corrosion protection of a transparent coating system containing particles of zinc compounds applied on steel sheets for enameling. Sarli et al. [54] applied polyurethane-based polymeric films on pretreated electrogalvanized steel which provided very effective protection against corrosion as a result of their excellent barrier properties. Gao et al. [55] studied acrylic coatings composed of modified MoS_2 nanosheets successfully prepared on the surface of galvanized sheets. Their results showed that modified MoS_2 nanosheets reduced the number of cracks in the coatings and made the coatings more compact. Furthermore, the coating's corrosion resistance was significantly enhanced. Li et al. [56] clarified the roles of titanium-containing materials in improving coatings when studying organic–inorganic hybrid coatings. As Kuznetsov analyzed [57], appropriately selected inhibitors will form a durable protective layer on the surface, preventing the formation of corrosion.

5. Conclusions

Based on this study's findings, it can be concluded that the tested sheet metal specimens with the TOC based on hydroxyl resins dissolved in water showed the most suitable lubrication properties due to the continuous coating layer compared to the other tested specimens. The lowest friction coefficient when measured by using the cup test in dry conditions resulted in lower drawing forces.

The dependence of the deep drawing force on the blank holding force is linear, and thanks to the special TOC surface treatment, the coefficient of friction was reduced from 0.119 to 0.053, which is more than half.

Good adhesion of the TOC was observed at each level of the blank holding force. No elements of the coating adhered to the drawing tool's contact surfaces.

As proved by the corrosion test, GI + TOC showed enhanced corrosion properties. The time to white corrosion appearance was greater than 72 h, as required by the customer, or more than twice that when compared to the GI passivated surface.

Thus, using GI + TOC based on hydroxyl resins dissolved in water, Ti and Cr^{3+} without the addition of pressing oils as a lubricant has several advantages—cost savings, an ecological clean process, savings on pressing tools and equipment, a decreased maintenance time and also much better corrosion resistance. Potential industrial applications of the studied TOC lie in a wide range of industries (construction, electronics, air conditioning, appliances, etc.) where metal sheet processing using stamping operations is involved.

Author Contributions: Conceptualization, M.T. and S.N.; methodology, S.N., F.H. and V.K.; validation, S.N., F.H. and V.K.; formal analysis, J.M.K. and M.B.; data curation, S.N., F.H. and V.K.;

writing—original draft preparation, M.T. and S.N.; writing—review and editing, M.T. and S.N.; visualization, J.M.K. and M.B.; supervision, E.E.; project administration, E.E.; funding acquisition, E.E. All authors have read and agreed to the published version of the manuscript.

Funding: This study was funded by Vedecká grantová agentúra MŠVVaŠ SR a SAV, grant number VEGA 1-0238-23.

Data Availability Statement: The data are only available on request due to restrictions provided by the funder.

Acknowledgments: This study was accomplished under the grant project VEGA 1-0238-23 "Implementation of CAx systems and virtual engineering techniques in the redesign of car-body parts for deformation zones".

Conflicts of Interest: Authors Stanislav Németh, František Hollý and Vladimír Kundracik are employed by the company U.S. Steel Košice s.r.o. The remaining authors declare that the research was conducted in the absence of any commercial or financial relationships that could be construed as a potential conflict of interest.

References

1. Čada, R. Formability of Deep-Drawing Steel Sheets. In Proceedings of the 5th European Conference on Advanced Materials and Processes and Applications (EUROMAT 97): Materials, Functionality Design: Volume 4-Characterization and Production/Design, Maastricht, The Netherlands, 21–23 April 1997; Netherlands Society for Materials Science: Maastricht, The Netherlands, 1997; pp. 463–466, ISBN 90-803513-4-2.
2. Liewald, M.; Wagne, S.; Becker, D. Influence of surface topography on the tribological behaviour of aluminium alloy 5182 with EDT surface. *Tribol. Lett.* **2010**, *39*, 135–142. [CrossRef]
3. Do, T.T.; Minh, P.S.; Le, N. Effect of Tool Geometry Parameters on the Formability of a Camera Cover in the Deep Drawing Process. *Materials* **2021**, *14*, 3993. [CrossRef] [PubMed]
4. Hazrati, J.; Stein, P.; Kramer, P.; van den Boogaard, A.H. Tool Texturing for Deep Drawing Applications. *IOP Conf. Ser. Mater. Sci. Eng.* **2018**, *418*, 012095. [CrossRef]
5. Šugárová, J.; Šugár, P.; Frnčík, M.; Necpal, M.; Moravčíková, J.; Kusý, M. The influence of the tool surface texture on friction and the surface layers properties of formed component. *Adv. Sci. Technol. Res. J.* **2018**, *12*, 181–193. [CrossRef] [PubMed]
6. Hou, J.; Deng, P.; Wang, S.; Xu, H.; Shi, Y. Study on formability and microstructure evolution of hot deep drawing manufactured 7005 aluminum alloy sheet metal. *Mater. Today Commun.* **2023**, *36*, 106794. [CrossRef]
7. Mihaliková, M.; Zgodavová, K.; Bober, P.; Špegárová, A. The Performance of CR180IF and DP600 Laser Welded Steel Sheets under Different Strain Rates. *Materials* **2021**, *14*, 1553. [CrossRef] [PubMed]
8. Feng, Y.; Hong, Z.; Gao, Y.; Lu, R.; Wang, Y.; Tan, J. Optimization of variable blank holder force in deep drawing based on support vector regression model and trust region. *Int. J. Adv. Manuf. Technol.* **2019**, *105*, 4265–4278. [CrossRef]
9. Kirkhorn, L.; Bushlya, V.; Andersson, M.; Stahl, J.-E. The influence of tool microstructure on friction in sheet metal forming. *Wear* **2013**, *302*, 1268–1278. [CrossRef]
10. Thipprakmas, S.; Sriborwornmongkol, J.; Jankree, R.; Phanitwong, W. Application of an Oleophobic Coating to Improve Formability in the Deep-Drawing Process. *Lubricants* **2023**, *11*, 104. [CrossRef]
11. Lange, K. *Handbook of Metal Forming*, 2nd ed.; Society of Manufacturing Engineers: Millersville, PA, USA, 1995.
12. Hrivnak, A.; Evin, E. *Formability of Steel Sheets*, 1st ed.; Elfa: Košice, Slovakia, 2004.
13. Chen, D.; Zhao, C.; Chen, X.; Li, H.; Zhang, X. Research on the active pressurized forced lubrication deep drawing process and evaluation of the lubrication effect. *Int. J. Adv. Manuf. Technol.* **2022**, *120*, 2815–2826. [CrossRef]
14. Bay, N.; Azushima, A.; Groche, P.; Ishibashi, I.; Merklein, M.; Morishita, M.; Nakamura, T.; Schmid, S.; Yoshida, M. Environmentally benign tribo-systems for metal forming. *CIRP Ann.* **2010**, *59*, 760–780. [CrossRef]
15. Reichardt, G.; Henn, M.; Reichle, P.; Umlauf, G.; Riedmüller, K.; Weber, R.; Barz, J.; Liewald, M.; Graf, T.; Tovar, G.E.M. Friction and wear behavior of deep drawing tools using volatile lubricants injected through laser-drilled micro-holes. *JOM* **2022**, *74*, 826–836. [CrossRef]
16. Jivan, R.; Eskandarzade, M.; Bewsher, S.; Leighton, M.; Mohammadpour, M.; Saremi-Yarahmadi, S. Application of solid lubricant for enhanced frictional efficiency of deep drawing process. Proceedings of the Institution of Mechanical Engineers. *Part C J. Mech. Eng. Sci.* **2022**, *236*, 624–634. [CrossRef]
17. European Commission. *Directorate-General for Research and Innovation*; Ferrari, V., Nicolle, R., Eds.; New surface treatment to improve adhesion of organic coatings and corrosion—In situ methods for the characterisation of Zn polymer coatings—Final report; Publications Office: Luxembourg, 2002.
18. European Commission. *Directorate-General for Research and Innovation*; Hardy, Y., Wormuth, R., Barranco Asensio, V., Eds.; New chromium-free thin organic coatings for Z, ZA and ZF—Final report; Publications Office: Luxembourg, 2003.
19. Trzepiecinski, T. A Study of the Coefficient of Friction in Steel Sheets Forming. *Metals* **2019**, *9*, 988. [CrossRef]

20. Padmanabhan, R.; Oliveira, M.C.; Alves, J.L.; Menezes, L.F. Influence of Process Parameters on the Deep Drawing of Stainless Steel. *Finite Elem. Anal. Des.* **2007**, *43*, 1062–1067. [CrossRef]
21. Zhao, H.; Cao, L.; Wan, Y.; Yang, S.; Gao, J.; Pu, J. Enhanced lubricity of zinc phosphate coating by stearic acid. *Lubr. Sci.* **2018**, *30*, 331–337. [CrossRef]
22. Bexell, U.; Carlsson, P.; Olsson, A. Tribological characterisation of an organic coating by the use of ToF-SIMS. *Appl. Surf. Sci.* **2003**, *203*, 596–599. [CrossRef]
23. Ma, I.A.W.; Ammar, S.; Kumar, S.S.A.; Ramesh, K.; Ramesh, A. A concise review on corrosion inhibitors: Types, mechanisms and electrochemical evaluation studies. *J. Coat. Technol. Res.* **2022**, *19*, 241–268. [CrossRef]
24. Lessa, R.C.d.S. Synthetic Organic Molecules as Metallic Corrosion Inhibitors: General Aspects and Trends. *Organics* **2023**, *4*, 232–250. [CrossRef]
25. Bammel, B.D.; Comoford, J.; Donaldson, G.T.; McGee, J.D.; Smith, T.S., II; Zimmerman, J. Novel Non-Chrome Thin Organic Hybrid Coating for Coil Steels. In Proceedings of the 38th Annual Waterborne Symposium, New Orleans, LA, USA, 28 February–4 March 2011; pp. 44–58.
26. Roos, O. Brugal® thin organic coatings: Effective and gainful alternative to traditional methods of protection of steels from corrosion. *Met. Sci. Heat Treat.* **2011**, *53*, 350–352. [CrossRef]
27. Thin Organic Coating. Available online: https://www.usske.sk/en/products/hot-dip-galvanized/thin-organic-coating (accessed on 3 March 2024).
28. Multiface®. Available online: https://www.voestalpine.com/surface-treatments/en/Products/Surface-treatments/multiface-R (accessed on 3 March 2024).
29. Easyfilm®. Available online: https://industry.arcelormittal.com/catalogue/E80/EN (accessed on 3 March 2024).
30. Directive 2011/65/EU of the European Parliament and of the Council of 8 June 2011 on the Restriction of the Use of Certain Hazardous Substances in Electrical and Electronic Equipment. Available online: http://data.europa.eu/eli/dir/2011/65/oj (accessed on 1 April 2024).
31. Carlsson, P.; Bexel, U.; Olsson, M. Friction and wear mechanisms of thin organic permanent coatings deposited on hot-dip coated steel. *Wear* **2001**, *247*, 88–99. [CrossRef]
32. Barletta, M.; Gisario, A.; Puopolo, M.; Vesco, S. Scratch, wear and corrosion resistant organic inorganic hybrid materials for metals protection and barrier. *Mater. Des.* **2015**, *69*, 130–140. [CrossRef]
33. Tsai, P.-Y.; Chen, T.-E.; Lee, Y.-L. Development and Characterization of Anticorrosion and Antifriction Properties for High Performance Polyurethane/Graphene Composite Coatings. *Coatings* **2018**, *8*, 250. [CrossRef]
34. Ying, L.; Wu, Y.; Nie, C.; Wu, C.; Wang, G. Improvement of the Tribological Properties and Corrosion Resistance of Epoxy–PTFE Composite Coating by Nanoparticle Modification. *Coatings* **2021**, *11*, 10. [CrossRef]
35. Trzepiecinski, T.; Lemu, H.G. Effect of Lubrication on Friction in Bending under Tension Test-Experimental and Numerical Approach. *Metals* **2020**, *10*, 544. [CrossRef]
36. Evin, E.; Daneshjo, N.; Mareš, A.; Tomáš, M.; Petrovčiková, K. Experimental Assessment of Friction Coefficient in Deep Drawing and Its Verification by Numerical Simulation. *Appl. Sci.* **2021**, *11*, 2756. [CrossRef]
37. Heinzel, H.; Ramezani, M.; Neitzert, T. Experimental Investigation of the Formability of Organic Coated Steel Sheet Metal. *Procedia Manuf.* **2015**, *1*, 854–865. [CrossRef]
38. Evin, E.; Tomáš, M. Influence of Friction on the Formability of Fe-Zn-Coated IF Steels for Car Body Parts. *Lubricants* **2022**, *10*, 297. [CrossRef]
39. Xia, J.; Zhao, J.; Dou, S.; Shen, X. A Novel Method for Friction Coefficient Calculation in Metal Sheet Forming of Axis-Symmetric Deep Drawing Parts. *Symmetry* **2022**, *14*, 414. [CrossRef]
40. Evin, E.; Németh, S.; Výrostek, M. Evaluation of Friction Coefficient of Stamping. *Acta Mech. Slovaca* **2014**, *18*, 20–27. [CrossRef]
41. *EN 10346:2015*; Continuously hot-dip coated steel flat products—Technical delivery conditions. CEN-CENELEC Management Centre: Brussels, Belgium, 2015.
42. *ISO 6892-1:2019*; Metallic Materials—Tensile Testing—Part 1: Method of Test at Room Temperature. International Organization for Standardization: Geneva, Switzerland, 2019.
43. *ISO 10113:2020*; Metallic Materials—Sheet and Strip—Determination of Plastic Strain Ratio. International Organization for Standardization: Geneva, Switzerland, 2020.
44. *ISO 10275:2020*; Metallic Materials—Sheet and Strip—Determination of Tensile Strain Hardening Exponent. International Organization for Standardization: Geneva, Switzerland, 2020.
45. *ISO 9227:2022*; Corrosion Tests in Artificial Atmospheres—Salt Spray Test. International Organization for Standardization: Geneva, Switzerland, 2022.
46. Popic, J.P.; Jegdic, B.V.; Bajat, J.B.; Veljovic, D.; Stevanovic, S.I.; Miskovic-Stankovic, V.B. The effect of deposition temperature on the surface coverage and morphology of iron-phosphate coatings on low carbon steel. *Appl. Surf. Sci.* **2011**, *257*, 10855–10862. [CrossRef]
47. Hara, A.; Kazimierczak, H.; Bigos, A.; Świątek, Z.; Ozga, P. Effect of different organic additives on surface morphology and microstructure of Zn-Mo coatings electrodeposited from citrate baths. *Arch. Metall. Mater.* **2019**, *64*, 207–220. [CrossRef]
48. Liu, X.; Yu, W.; Zhang, Q.; Jiang, S. Influence of Surface Roughness of Galvanized Steel Sheet on Self-lubricated Coating. *J. Iron Steel Res. Int.* **2014**, *21*, 342–347. [CrossRef]

49. Sankara Narayanan, T.S.N. Surface Pretreatment by Phosphate Conversion Coatings—A Review. *Rev. Adv. Mater. Sci.* **2005**, *9*, 130–177.
50. Shih, H. Friction and Die Wear in Stamping Prephospated Advanced High Strength Steels. *SAE Int. J. Mater. Manf.* **2016**, *9*, 481–487. [CrossRef]
51. Saffarzade, P.; Ali Amadeh, A.; Agahi, N. Study of tribological and friction behavior of magnesium phosphate coating and comparison with traditional zinc phosphate coating under dry and lubricated conditions. *Tribol. Int.* **2020**, *144*, 106122. [CrossRef]
52. Carlsson, P.; Bexel, U.; Olsson, M. Tribological behaviour of thin organic permanent coatings deposited on hot-dip coated steel sheet—A laboratory study. *Surf. Coat. Technol.* **2000**, *132*, 169–180. [CrossRef]
53. Podjuklová, J.; Laník, T.; Hrabovská, K.; Bártek, V.; Suchánková, K.; Kopaňáková, S.; Šrubař, P.; Dvorský, R. Study on thin organic coatings for short-term anticorrosive protection of metallurgical materials production. In Proceedings of the 20th Anniversary International Conference on Metallurgy and materials, Brno, Czech Republic, 18–20 May 2011.
54. Sarli, A.R.D.; Elsner, C.I.; Tomachuk, C.R. Characterization and Corrosion Resistance of Galvanized Steel/Passivation Composite/Polyurethane Paint Systems. *Curr. J. Appl. Sci. Technol.* **2013**, *4*, 853–878. [CrossRef]
55. Gao, F.; Du, A.; Ma, R.; Lv, C.; Yang, H.; Fan, Y.; Zhao, X.; Wu, J.; Cao, X. Improved corrosion resistance of acrylic coatings prepared with modified MoS2 nanosheets. *Colloids Surf. A Physicochem. Eng. Asp.* **2020**, *587*, 124318. [CrossRef]
56. Li, H.; Sun, L.; Li, W. Application of organosilanes in titanium-containing organic–inorganic hybrid coatings. *J. Mater. Sci.* **2022**, *57*, 13845–13870. [CrossRef]
57. Kuznetsov, Y.I.; Redkina, G.V. Thin Protective Coatings on Metals Formed by Organic Corrosion Inhibitors in Neutral Media. *Coatings* **2022**, *12*, 149. [CrossRef]

Disclaimer/Publisher's Note: The statements, opinions and data contained in all publications are solely those of the individual author(s) and contributor(s) and not of MDPI and/or the editor(s). MDPI and/or the editor(s) disclaim responsibility for any injury to people or property resulting from any ideas, methods, instructions or products referred to in the content.